NASA TECHNICAL NOTE

NASA TN D-7415

NASA TN D-7415

POSTFLIGHT SIMULATION OF PARACHUTE DEPLOYMENT DYNAMICS OF VIKING QUALIFICATION FLIGHT TESTS

by Charles H. Whitlock, Lamont R. Poole, and Theodore A. Talay

Langley Research Center
Hampton, Va. 23665

NATIONAL AERONAUTICS AND SPACE ADMINISTRATION • WASHINGTON, D. C. • SEPTEMBER 1973

1. Report No.	2. Government Accession No.	3. Recipient's Catalog No.
NASA TN D-7415		

4. Title and Subtitle	5. Report Date
POSTFLIGHT SIMULATION OF PARACHUTE DEPLOYMENT DYNAMICS OF VIKING QUALIFICATION FLIGHT TESTS	September 1973
	6. Performing Organization Code

7. Author(s)	8. Performing Organization Report No.
Charles H. Whitlock, Lamont R. Poole, and Theodore A. Talay	L-9145
	10. Work Unit No.
9. Performing Organization Name and Address	815-20-09-01
NASA Langley Research Center Hampton, Va. 23665	11. Contract or Grant No.
	13. Type of Report and Period Covered
12. Sponsoring Agency Name and Address	Technical Note
National Aeronautics and Space Administration Washington, D.C. 20546	14. Sponsoring Agency Code

15. Supplementary Notes

16. Abstract

Simulation calculations of the Viking qualification flight tests are conducted by use of analytical models of the parachute deployment dynamics process. Results from the study indicate that good simulations of event times and trajectory are obtained. If the full-scale parachute drag coefficient is used, a good simulation of first opening load is obtained and the overall nature of the load history is calculated. For longitudinal motions, the two-degree-of-freedom models give good agreement with a six-degree-of-freedom model. It is believed that the analytical models used are tools which will aid in the analysis of future flight systems.

17. Key Words (Suggested by Author(s))	18. Distribution Statement
Parachutes Parachute deployment Parachute analytical models	Unclassified – Unlimited

19. Security Classif. (of this report)	20. Security Classif. (of this page)	21. No. of Pages	22. Price*
Unclassified	Unclassified	36	Domestic, $3.00 Foreign, $5.50

*For sale by the National Technical Information Service, Springfield, Virginia 22151

POSTFLIGHT SIMULATION OF PARACHUTE DEPLOYMENT DYNAMICS OF VIKING QUALIFICATION FLIGHT TESTS

By Charles H. Whitlock, Lamont R. Poole, and Theodore A. Talay
Langley Research Center

SUMMARY

Simulation calculations of the Viking qualification flight tests are conducted by use of analytical models of the parachute deployment dynamics process. Results from the study indicate that good simulations of event times and trajectory are obtained. If the full-scale parachute drag coefficient is used, a good simulation of first opening load is obtained and the overall nature of the load history is calculated. For longitudinal motions, the two-degree-of-freedom models give good agreement with a six-degree-of-freedom model. It is believed that the analytical models used are tools which will aid in the analysis of future flight systems.

INTRODUCTION

It is always a question as to how well an analytical model can simulate actual flight events. In the case of parachute deployment, accurate simulation is difficult because inflation from a tightly folded condition is not precisely repeatable. The designer, faced with the task of predicting deployment dynamics for a future mission, may be forced to use analytical techniques to study both nominal and dispersed inflation characteristics. In order for the designer to have confidence in such an analysis, the analytical models used should have previously been successful in simulating actual flight results.

In support of the Viking Project, analytical models of the decelerator deployment process have been developed at the Langley Research Center. The models are described in detail in references 1 to 3. The physical phenomena considered as well as the differences between the various models are summarized in reference 4. The purpose of this paper is to evaluate the simulation capabilities and limitations of these models by comparing calculated and flight results for conditions actually experienced in a series of flight tests. Specifically, analytically simulated histories of separation distance, Mach number, dynamic pressure, and loads will be compared with flight values.

This study will limit itself to simulation calculations of previous flight events. Actual flight values for filling characteristics (canopy frontal-area growth history) will be used. However, all other aerodynamic and physical property data (with the exception

of parachute drag coefficient) used for model input will be those values which were obtained from wind-tunnel and laboratory tests prior to flight. By using data which could be obtained prior to flight, it is expected that an understanding of model limitations for the prediction of future missions will be obtained.

SYMBOLS

a/b	body dimensions, prolate ellipsoid
D_o	nominal diameter, meters (feet)
h	canopy cylinder height, meters (feet)
K'	apparent mass coefficient
L/D	lift-drag ratio
m	mass, kilograms (slugs)
$\dot{m}$	time rate of change of mass, kilograms/second (slugs/second)
n	exponent
R	radius, meters (feet)
V	volume, meters^3 (feet^3)
ρ	density, kilograms/meter^3 (slugs/foot^3)

Subscripts:

app	apparent
fi	full inflation
inc	included
∞	free stream

FLIGHT TESTS

System Description

The Viking parachute qualification effort consisted of two series of flight tests as shown in figure 1. Test parachutes for the balloon-launched decelerator tests (BLDT) were deployed at altitudes between 26 526 meters (87 027 ft) and 44 862 meters (147 186 ft). Three successful tests at Mach numbers of 0.47, 1.13, and 2.13 were conducted at dynamic pressures between 239 and 522 N/m^2 (5.0 and 10.9 lb/ft^2). The low-altitude qualification test (LAQT) vehicles were launched from aircraft at altitudes of approximately 14 500 meters (47 500 ft). Two successful tests were conducted at a Mach number of 0.25 and at dynamic pressures of 642 and 647 N/m^2 (13.4 and 13.5 lb/ft^2), respectively.

The test vehicle for the BLDT system is described in detail in reference 5 and was basically a blunted 70^o half-angle cone 3.5 meters (11.5 ft) in diameter weighing approximately 8000 newtons (1800 lb). A center-of-gravity offset from the center line was used to produce a lifting capability with an L/D range of 0.135 ± 0.015. Angle of attack was not precisely controlled at the beginning of deployment, but ranged from 5.2^o to 7.3^o depending upon flight. Data from the BLDT tests are given in references 6 to 9.

The test vehicle for the LAQT system is described in reference 10 and was a 0.7-meter (2.3-ft) maximum diameter flared cylinder which weighed 12 670 newtons (2850 lb). Angle of attack at deployment was not monitored.

The parachute systems were identical for both BLDT and LAQT except for bridle length and are described in references 9 and 11. The canopy had a 16.5-meter (53-ft) nominal diameter and was a disk-gap-band configuration. The 48 gore parachute used suspension lines which were 27.4 meters (90 ft) in length prior to flight. The parachute was attached to the payload by means of a connecting swivel and a three-leg bridle. The swivel was located aft of the test vehicle at the juncture of the suspension lines and bridle legs and was used to reduce spin coupling between the parachute and the test vehicle. Weight of the parachute-swivel-bridle system was approximately 430 newtons (97 lb).

Deployment Sequence

The Viking parachute is mortar-ejected with a lines-first technique of deployment as shown in figure 2. For purposes of this investigation, the deployment process is defined to include both the unfurling and inflation phases so that consideration is given to the total dynamic process between parachute ejection and attainment of a stable parachute configuration. The unfurling phase considers the process from ejection until the parachute is fully extended behind the vehicle. The inflation phase considers both the initial

canopy growth to full projected diameter and the breathing motions (variations in parachute frontal area) which occur just following inflation and before the achievement of a stable canopy configuration.

MODEL INPUT

Input to the analytical models consists of physical properties, aerodynamic coefficients, initial conditions, and the canopy inflation history. All inputs were taken from laboratory and ground facility sources except for parachute drag coefficient and canopy inflation history. Scale effects between wind-tunnel parachute data and full-size results are known to exist because of flow interaction effects and the inability to scale cloth thickness, permeability, and stiffness. As a result, full-scale parachute drag coefficient and projected-area histories were used for simulation calculations to test the validity of the computer models. Sources of the various input data are described.

Physical Properties

Test-vehicle mass, center of gravity, and inertia values were taken from measurements by the manufacturer. Bridle, suspension-line, and canopy mass and center-of-gravity values were also obtained from manufacturer's measurements and drawings. These data were used to compute the mass distribution along the "strung-out" length which was a required input. Parachute inertia values, if needed, were computed internal to the program as a function of projected area based on input values of mass and center of gravity for various components of the canopy and computed values of included and apparent mass.

Suspension-system properties were obtained from laboratory tensile tests. Nonlinear suspension-line elastic and damping properties were used as reported in reference 12. Nonlinear elastic properties for the bridle legs were obtained from the manufacturer. The bridle was overdesigned and experiences low values of elongation and elongation rate in comparison to the suspension lines during the deployment process. Bridle-leg damping values were unavailable; therefore, zero viscous damping was assumed. This assumption is not expected to present a serious deficiency to the simulation study.

Aerodynamic Coefficients

Test-vehicle aerodynamic coefficients for the BLDT simulations were obtained by wind-tunnel measurements. Wind-tunnel data were not available for the LAQT test vehicle; therefore, input values based on data from similar configurations were estimated.

Parachute drag coefficients were taken from average values of all full-scale test flights. Initial simulations were based on wind-tunnel parachute data. These simulations

produced correct trends but incorrect magnitudes. The problem was that the small-scale tunnel models produced lower drag coefficients at supersonic velocities than the full-scale tests. (See ref. 11.) Drag coefficient values used for this study are shown in figure 3. Parachute stability coefficients were not required for simulation of longitudinal dynamics.

Initial Conditions

Trajectory conditions for beginning the forward-running simulation calculations were taken from flight data. Three BLDT flights (known as AV-2, AV-3, and AV-4) and two LAQT flights (known as LAQT-2 and LAQT-3) were simulated. BLDT AV-1 and LAQT-1 were not simulated because of hardware failures in those flights. (See refs. 10 and 11.) Initial conditions at mortar fire for each simulation are given below:

	Flight				
	AV-2	AV-3	AV-4	LAQT-2	LAQT-3
Velocity, m/sec (ft/sec)	364 (1194)	141 (464)	698 (2290)	75.9 (249)	74.1 (243)
Dynamic pressure, N/m^2 (lb/ft^2) . .	239 (5.00)	330 (6.90)	522 (10.90)	642 (13.40)	647 (13.52)
Flight path angle, deg	12.5	-89.5	12.3	-90	-90
Ejection velocity, m/sec (ft/sec) . .	32.9 (108)	32.9 (108)	35.1 (115)	33.5 (110)	32.6 (107)

Ejection velocities were deduced from parametric studies in which the event time for line stretch was calculated over a range of velocities by use of the model of reference 1. Final simulation calculations used these values which provided best agreement with flight events.

Canopy Inflation

The history of canopy projected area is a critical input parameter during the inflation process. It describes the filling sequence and timing as well as breathing motions prior to the achievement of a stable canopy. For prediction of future flights, the projected-area history would be subject to parametric variation based on previous full-scale flight experience concerning inflation repeatability. To simulate a particular flight, however, it is necessary to input the actual history experienced on that flight. Since the purpose of this study is to determine simulation capability of the analytical modeling, detailed projected-area histories taken from camera data were input to the program for each particular flight.

STUDY LIMITATIONS

Plastic Deformation

Unpublished tests with the Viking suspension lines have shown that if the material is loaded in tension to 25 percent of its ultimate load and unloaded back to zero over a

25-second time interval, then the lines will have a plastic set of approximately 2.5 percent. More important, on the unloading or return stroke, both the slope and shape of the force-elongation curve are different from those of the initial load stroke. This condition implies that plastic set has the effect of changing both elasticity and damping values when many repeated oscillations occur in the suspension system. An additional problem is that plastic deformation is known to be a function of time as well as of stress. The load cycle which takes 25 seconds in the laboratory occurs in less than 1 second during a typical BLDT flight. The effects of plastic set under such rapid loading conditions are not known at the present time. For this reason, the elasticity and damping values of reference 12 (taken during loading strokes only) are assumed to be valid for both the loading and unloading phases of the oscillations. This assumption has the effect of producing valid elastic properties during canopy growth to first full inflation, but causes some errors of unknown magnitude during subsequent breathing motions.

Flow Interactions

The simulation calculations also do not consider the detailed effects of unsteady flow interactions associated with a breathing canopy. The aerodynamic interactions of a breathing parachute immersed in the wake of a large-diameter body are not quantitatively understood. Reference 13 shows basic wake characteristics without a trailing parachute. The wake data correlate with the overall trend of the parachute drag data (ref. 14); however, detailed drag predictions are not possible because insertion of a parachute into the wake creates an additional shock in front of the canopy mouth. This shock, in turn, influences and disturbs the surrounding wake. The rates of mass inflow and outflow are affected; as a result, the drag produced by the canopy changes. If the canopy mouth is breathing, then the interaction between the parachute and the wake is unsteady.

The problem is further compounded if free-stream Mach number is changing rapidly during flight. In reality, the drag coefficient of the parachute is a function of Mach number, angle of attack, projected area (or parachute profile), longitudinal wake location, and radial displacement from the wake center line. The specific variation of drag with all of these parameters cannot be deduced from existing data. To bypass this problem, parachute tension measurements have been averaged and used with free-stream dynamic pressure and nominal canopy area when conversion is made to drag coefficient values. The drag coefficients then include average wake and projected-area effects.

For purposes of this simulation study, drag coefficient is assumed to be a function of Mach number only. Free-stream dynamic pressure, nominal canopy area, and the ratio of instantaneous projected area to full-open projected area are used to compute instantaneous parachute drag force. These approximations to the actual unsteady conditions are expected to reproduce the overall nature of the load history.

Study Depth

It should be noted that in-depth simulations could be accomplished by using iterative techniques to make parametric variations of the unknown quantities until detailed agreement is obtained. For example, suspension-system elasticity and damping could be varied until "best fit" effective values which account for the integrated effect of plastic deformation are obtained. Also, parachute drag coefficient could be modified by numerous arbitrary functions of projected area and wake location until best-fit conditions are achieved. The results of such an in-depth study would be of value in that trends in the variation of the parameters would be established. However, the designer of a future mission would not normally possess such in-depth information for prediction purposes. At best, he would probably only have drag coefficients from flight tests of other systems which used the same canopy configuration and suspension-system elastic and damping properties obtained from laboratory tensile tests. For this reason, this simulation study will limit itself to the use of full-scale parachute drag coefficient values and other data that could be obtained in laboratory or wind-tunnel tests.

RESULTS AND DISCUSSION

Figure 4 shows simulation histories and flight data for separation distance for each of the BLDT and LAQT flight tests. The solid line in each figure represents the distance between the deployment bag and the test vehicle as computed by the technique of reference 1. The dashed line represents distance from the vehicle to the bottom of the canopy skirt. Suspension-system elongation and longitudinal oscillation during canopy growth and breathing as computed by use of the reference 2 model are shown. Event times actually experienced during the flights are shown by circular symbols. The event of line stretch was clearly recorded on telemetry data and flight photographs, but bag strip time is often unknown because there is no abrupt change in load to signify the event. Also, the canopy crown is sometimes hidden from camera view by the partially inflated canopy mouth. The canopy crown was visible in the film data from the BLDT AV-2 and AV-4 tests, and estimates of bag strip times were made for these flights. (See refs. 6 and 8.) Review of results for these flights indicates that the reference 1 model provides good simulation of unfurling distance and event times. Flight data are not available to verify the suspension-system longitudinal oscillation values.

Figure 5 shows Mach number and dynamic-pressure results from trajectory simulation calculations for the various flights. Symbols indicate flight data, and uncertainty bands are shown to note tracking and data reduction accuracies. Both the reference 1 and reference 2 models utilize the 1962 standard atmosphere. Atmospheric properties for each flight differed from standard values because of geographical differences and weather variations. To allow analytical simulation, velocity and dynamic-pressure values from

the flight data were used for initial conditions. Actual flight altitude was not simulated but was adjusted to provide matched velocity and dynamic pressure. An additional result of such a procedure is that temperature and speed of sound are not simulated; thus, errors in Mach number result as shown in figure 5. The errors however are generally within the accuracy of the tracking data. Review of results for all the flights indicates that dynamic-pressure variation during deployment (finite-mass effect) is well simulated by the reference 1 and reference 2 models over a wide range of conditions.

Figure 6 shows the simulation of parachute loads during deployment. Both analytical and flight results are shown for suspension-system tension. Analytical results also show the drag force produced by the canopy. Parachute drag force histories are not available from flight data. Comparison of results for all the flights indicates that the overall nature of the load histories is simulated.

Analytical calculations were made in which suspension-line elasticity and damping were varied and parachute drag coefficient was assumed to be an arbitrary function of projected area. Results show that suspension-line properties and parachute drag coefficient are important parameters which significantly influence oscillation calculations during the canopy breathing phase. Improved state-of-the-art knowledge of input data in these areas should improve the accuracy of the simulation calculations. For many deployments, suspension-line damping is an important parameter. Reference 12 shows the damping coefficient to be a nonlinear function of both strain and strain rate. This study found that it was particularly important that damping values from the correct strain-rate environment be used in the calculations. It was also found that large errors in the low-altitude simulation occur if the effect of time rate of change of included and apparent mass is ignored during the inflation process.

An item of particular interest is how well does the analytical modeling simulate the first opening load of the inflation process. The first opening load is important because it is usually the maximum load during deployment which, in turn, dictates the structural design and weight of the parachute. In addition, calculation of the first opening load is not limited by the lack of knowledge of suspension-system plastic deformation effects. Canopy growth until the first opening load involves only a single tensile elongation of the suspension system. Since the reference 12 data were obtained by use of tensile loading measurements, the elasticity and damping values from those tests are valid for the calculation of first opening load. It is during the return stroke and subsequent oscillations that plastic deformation is expected to influence suspension-system properties. Comparisons of analytical with experimental values of the first opening load are shown in figure 7. Agreement is approximately 10 percent for all flights.

One probable reason for the errors is uncertainty in the parachute drag coefficient data used as program input. Figure 3 shows the input drag coefficient curve which was faired from flight results. In the AV-2 case, inflation occurs in the transonic region where there is a steep gradient and a larger uncertainty in the drag coefficient history. Only a slight difference in the curve fairing in this region would produce better (or worse) agreement with flight opening-load values.

Another problem with the LAQT simulations is possible uncertainty in the calculation of included and apparent mass effects during inflation. No data are available for precise definition of included and apparent masses under the conditions of variable canopy geometry. Ignoring these terms completely causes a 25- to 30-percent error in the LAQT opening-load simulations. For this study, theoretical equations for included and apparent mass based on steady-state equations (ref. 15) and use of potential-flow theory (ref. 16) have been developed. Development of the included and apparent mass equations is given in the appendix.

From the BLDT and LAQT simulations, it is evident that a good calculation of the first opening load is not possible without an accurate knowledge of the full-scale parachute drag coefficient as well as suspension-system elastic and damping properties. For low-altitude flights, a good knowledge of included and apparent mass effects is also necessary.

Another item of interest is how well different analytical models compare when the same flight is simulated. All the previously discussed comparisons utilize the two-degree-of-freedom modeling techniques of references 1 and 2. Those models use Lagrangian mechanics type of modeling in which the equations of motion are defined for each body and then constraint equations which describe the nonlinearly elastic suspension system are used to couple the two bodies. The six-degree-of-freedom model of reference 3 utilizes a more sophisticated concept in which matrix displacement theory is used to calculate equilibrium positions in a spatial framework structure composed of the individual members of the suspension system. The forces and moments generated in the suspension system are then used in the equations of motion of the two bodies to determine the displacement for the subsequent equilibrium calculations. The six-degree-of-freedom modeling is much more complex than the two-degree-of-freedom technique, but has the advantage of considering nonsymmetric motion in each bridle leg and suspension-line group. Such capability is required if both bodies are each allowed to oscillate with the full six degrees of freedom. Such modeling must also be able to simulate the simplified longitudinal dynamics case without the effects of angular motion. Figure 8 shows a comparison of deployment loads computed by both the two-degree-of-freedom and the six-degree-of-freedom techniques for the BLDT AV-4 flight. Agreement between the two techniques is good in spite of differences in modeling and programing concepts.

CONCLUSIONS

A postflight study has been conducted to compare analytical simulation of parachute deployment dynamics with flight results obtained from Viking qualification tests. Based on the results of this study, the following conclusions are made with respect to the simulation of parachute deployments involving lines-first types of deployment systems similar to Viking:

1. The model of NASA TN D-6671 provides a good simulation of the unfurling motions required to predict event times.

2. The model of NASA TN D-6671 used in conjunction with the inflation model of NASA TM X-2592 provides a good simulation of both trajectory and the overall nature of the loads during deployment.

3. A good simulation of first opening load is obtained if full-scale parachute drag coefficient as well as suspension-system elastic and damping properties are known.

4. The two-degree-of-freedom techniques of NASA TN D-6671 and NASA TM X-2592 give good agreement with the six-degree-of-freedom model of AIAA Paper No. 73-460.

5. Better knowledge of (1) suspension-system material properties under dynamic loading conditions and (2) unsteady wake interaction-parachute drag characteristics would be expected to improve simulation results.

Based on these results, it is believed that these analytical models are tools which will aid the analysis of future flight systems. If separation distance, event times, trajectory, and loads are the only requirements, the two-degree-of-freedom modeling is recommended to minimize model complexity. If the vehicle system is sensitive to angular motions and rates, then six-degree-of-freedom modeling is necessary. Suspension-system elastic and damping properties from laboratory tests are a requirement. Full-scale parachute drag coefficients from other tests with similar canopy configurations should be utilized in the calculations to eliminate errors due to scale effects. Most important, the inflation history, in terms of the projected-area ratio, must be varied in a parametric manner to simulate the dispersions in filling time and breathing motions which occur between flights of identically designed systems. The results of such a parametric study would be the prediction of limits within which the flight results could be expected to occur. Given the knowledge of suspension-system elastic and damping properties, the models compute both drag force on the canopy and tension felt at the vehicle. This feature enables the models to be used in the analysis of test failures. Parametric

variation of parachute drag coefficient and inflation history may be used to calculate canopy loading by simulation of vehicle-measured forces. Definition of canopy drag loading may then allow more accurate stress calculations and analysis of failures.

Langley Research Center,
National Aeronautics and Space Administration,
Hampton, Va., August 27, 1973.

APPENDIX

INCLUDED AND APPARENT MASS CALCULATIONS

For the simulations conducted, the included air mass is taken to be that volume of air contained within the parachute canopy. For simplicity, a cylinder-hemisphere model is assumed for the canopy as shown in figure 9 where three stages of canopy inflation are depicted. At bag strip, no preinflation being assumed, the model canopy takes the shape of a long, thin cylinder. At any intermediate stage, the model canopy is a cylinder-hemisphere combination, whereas at full inflation it is assumed to be a hemisphere.

Based on this model, the volume of air, and hence the mass, included in the canopy may be calculated. The cylinder height is obtained by considering the definition of the nominal diameter. As seen in figure 9,

$$h = \frac{D_o - \pi R}{2} \tag{1}$$

The total volume enclosed by the canopy model is the volume of the cylinder plus the volume of the hemisphere, or,

$$V_{inc} = \pi R^2 h + \frac{2}{3}\pi R^3 \tag{2}$$

At full inflation $h = 0$ and the included volume is that of a hemisphere. The included air mass is given by

$$m_{inc} = V_{inc}\rho_\infty \tag{3}$$

where ρ_∞ is assumed to be free-stream air density for these simulations. Combining equations (2) and (3) yields

$$m_{inc} = \left(\pi R^2 h + \frac{2}{3}\pi R^3\right)\rho_\infty \tag{4}$$

When a parachute is decelerating, there is a net kinetic energy change in the surrounding air. The apparent mass of a parachute represents that mass that must be added to the actual mass of the parachute to represent the inertia of the surrounding air. There is a lack of definitive information about the apparent mass of an inflating parachute. However, by combining some results of potential flow theory and experiment, an estimation of this quantity can be made.

In the longitudinal direction the apparent mass is given by reference 15 as

$$m_{app} = K'\rho_\infty \pi R^3 \tag{5}$$

where ρ_∞ is the air density, and R is the canopy radius. The quantity K' is not a constant but varies as the canopy inflates. The quantity K' is also assumed to be a non-linear function of body geometry only, namely,

$$K' = K'_{fi}\left(\frac{a}{b}\right)^n \tag{6}$$

where K'_{fi} is the apparent mass coefficient at full inflation, a/b is related to the canopy dimensions, and n is some exponential power.

Potential flow theory (ref. 16) provides information such as the fact that a value for n can be deduced by assuming that the parachute at various stages of inflation resembles prolate ellipsoids. With this assumption, a value of $n = 4/3$ is obtained.

The ratio a/b is related to the dimensions of a prolate ellipsoid and can be approximated by

$$\frac{a}{b} = \frac{2R + h}{2R} \tag{7}$$

Based on a previous study, the value of K'_{fi} used in these simulations was calculated to be 0.74. This value is the present best estimate but not necessarily definitive. Substituting these values into equation (5) yields the equation for apparent mass as used in the simulations; that is,

$$m_{app} = 0.74\left(\frac{2R + h}{2R}\right)^{4/3} \pi R^3 \rho_\infty \tag{8}$$

The total included and apparent mass at any point in the inflation process is simply the sum of equations (4) and (8). The included and apparent mass rates $\dot{m}$ was calculated in the simulations as the time rate of change of the total included and apparent mass between successive integration steps.

REFERENCES

1. Poole, Lamont R.; and Huckins, Earle K., III: Evaluation of Massless-Spring Modeling of Suspension-Line Elasticity During the Parachute Unfurling Process. NASA TN D-6671, 1972.

2. Poole, Lamont R.: Computer Program for Investigating Effects of Nonlinear Suspension-System Elastic Properties on Parachute Inflation Loads and Motions. NASA TM X-2592, 1972.

3. Talay, Theodore A.; Morris, W. Douglas; and Whitlock, Charles H.: An Advanced Technique for the Prediction of Decelerator System Dynamics. AIAA Paper No. 73-460, May 1973.

4. Whitlock, Charles H.: Advances in Modeling Aerodynamic Decelerator Dynamics. Astronaut. & Aeronaut., vol. 11, no. 4, Apr. 1973, pp. 67-71.

5. Raper, James L.; Michel, Frederick C.; and Lundstrom, Reginald R.: The Viking Parachute Qualification Test Technique. AIAA Paper No. 73-456, May 1973.

6. Dickinson, D.; Schlemmer, J.; Hicks, F.; Michel, F.; and Moog, R. D.: Balloon Launched Decelerator Test Program Post-Test Test Program (45 Day) BLDT Vehicle AV-2. TR-3720291, Martin Marietta Corp., Dec. 15, 1972. (Available as NASA CR-112177.)

7. Dickinson, D.; Schlemmer, J.; Hicks, F.; Michel, F.; and Moog, R. D.: Balloon Launched Decelerator Test Program Post-Test Test Report (45 Day) BLDT Vehicle AV-3. TR-3720293, Martin Marietta Corp., Jan. 1973. (Available as NASA CR-112178.)

8. Dickinson, D.; Schlemmer, J.; Hicks, F.; Michel, F.; and Moog, R. D.: Balloon Launched Decelerator Test Program Post-Test Test Report (45 Day) BLDT Vehicle AV-4. TR-3720295, Martin Marietta Corp., Oct. 20, 1972. (Available as NASA CR-112179.)

9. Moog, R. D.; and Michel, F. C.: Balloon Launched Viking Decelerator Test Program Summary Report. TR-3720359, Martin Marietta Corp., Mar. 1973. (Available as NASA CR-112288.)

10. Murrow, H. N.; Henke, D. W.; and Eckstrom, C. V.: Development Flight Test of the Viking Decelerator System. AIAA Paper No. 73-455, May 1973.

11. Moog, R. D.; Bendura, R. J.; Timmons, J. D.; and Lau, R. A.: Qualification Flight Tests of the Viking Decelerator System. AIAA Paper No. 73-457, May 1973.

12. Poole, Lamont R.: Force-Strain Characteristics of Dacron Parachute Suspension-Line Cord Under Dynamic Loading Conditions. AIAA Paper No. 73-446, May 1973.

13. Campbell, James F.; and Brown, Clarence A., Jr.: Evaluation of Experimental Flow Properties in the Wake of a Viking '75 Entry Vehicle. AIAA Paper No. 73-475, May 1973.

14. Steinberg, Sy; Siemers, Paul M., III; and Slayman, Robert G.: Development of the Viking Parachute Configuration by Wind Tunnel Investigation. AIAA Paper No. 73-454, May 1973.

15. Amer. Power Jet Co.: Performance of and Design Criteria for Deployable Aerodynamic Decelerators. ASD-TR-61-579, U.S. Air Force, Dec. 1963. (Available from DDC as AD 429 921.)

16. Flügge, Wilhelm, ed.: Handbook of Engineering Mechanics. 1st ed., McGraw-Hill Book Co., Inc., 1962.

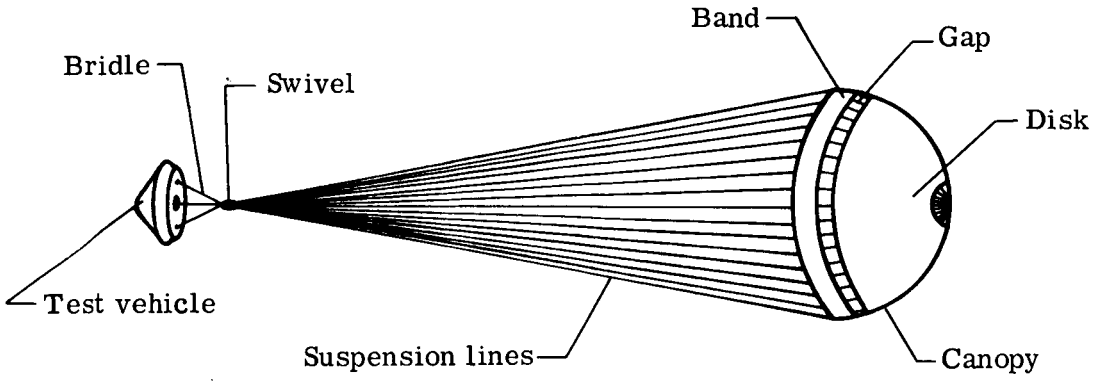

(a) Balloon-launched decelerator test (BLDT) configuration.

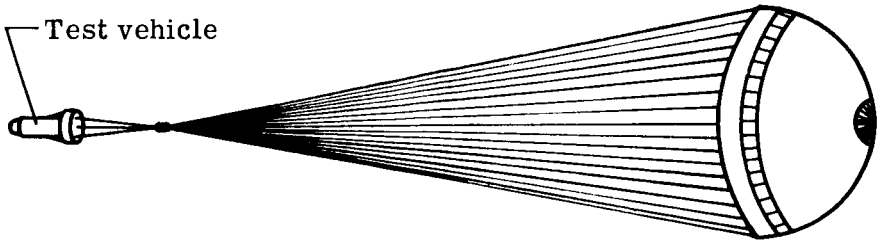

(b) Low-altitude qualification test (LAQT) configuration.

Figure 1.- System configurations for Viking parachute qualification flight tests.

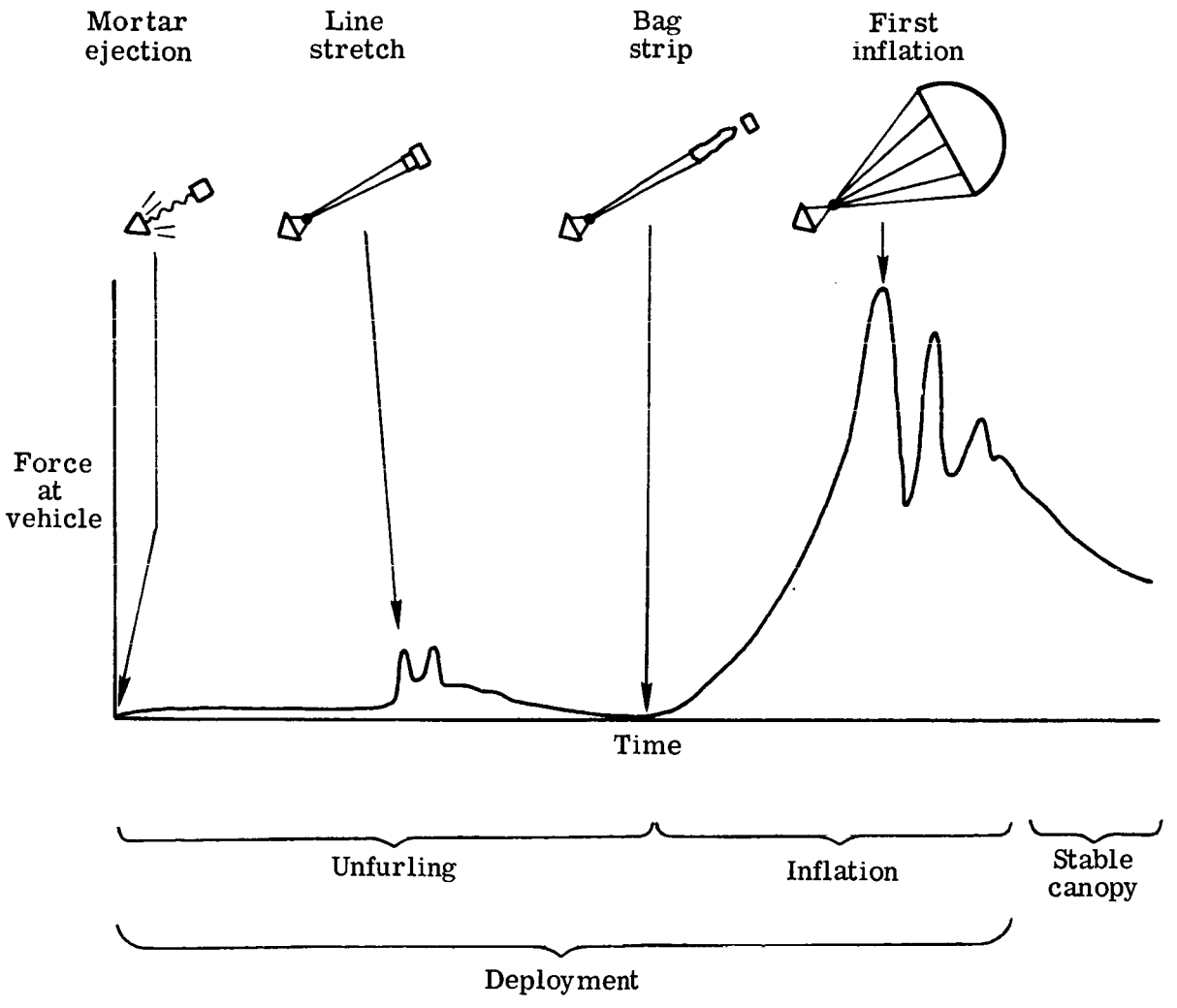

Figure 2.- Decelerator deployment sequence.

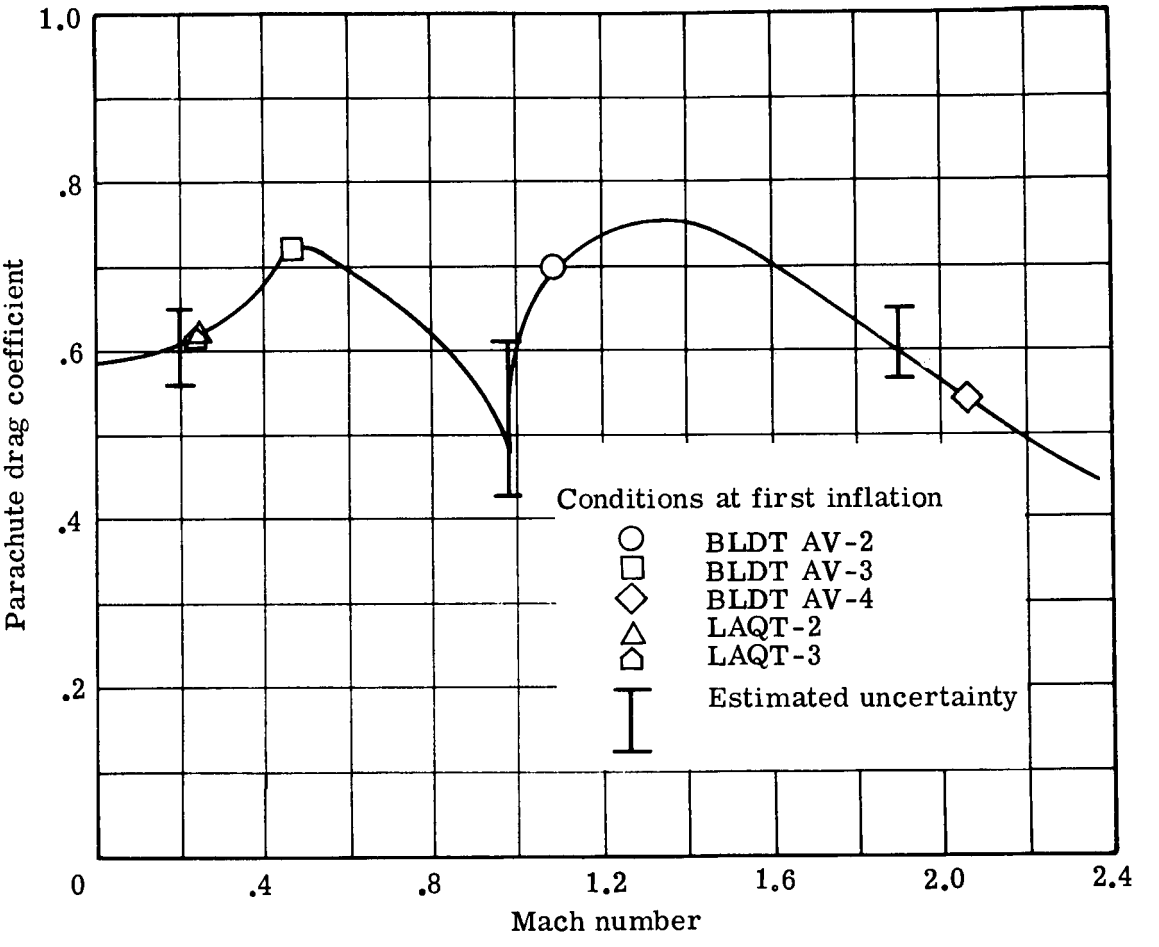

Figure 3.- Full-scale parachute drag coefficient.

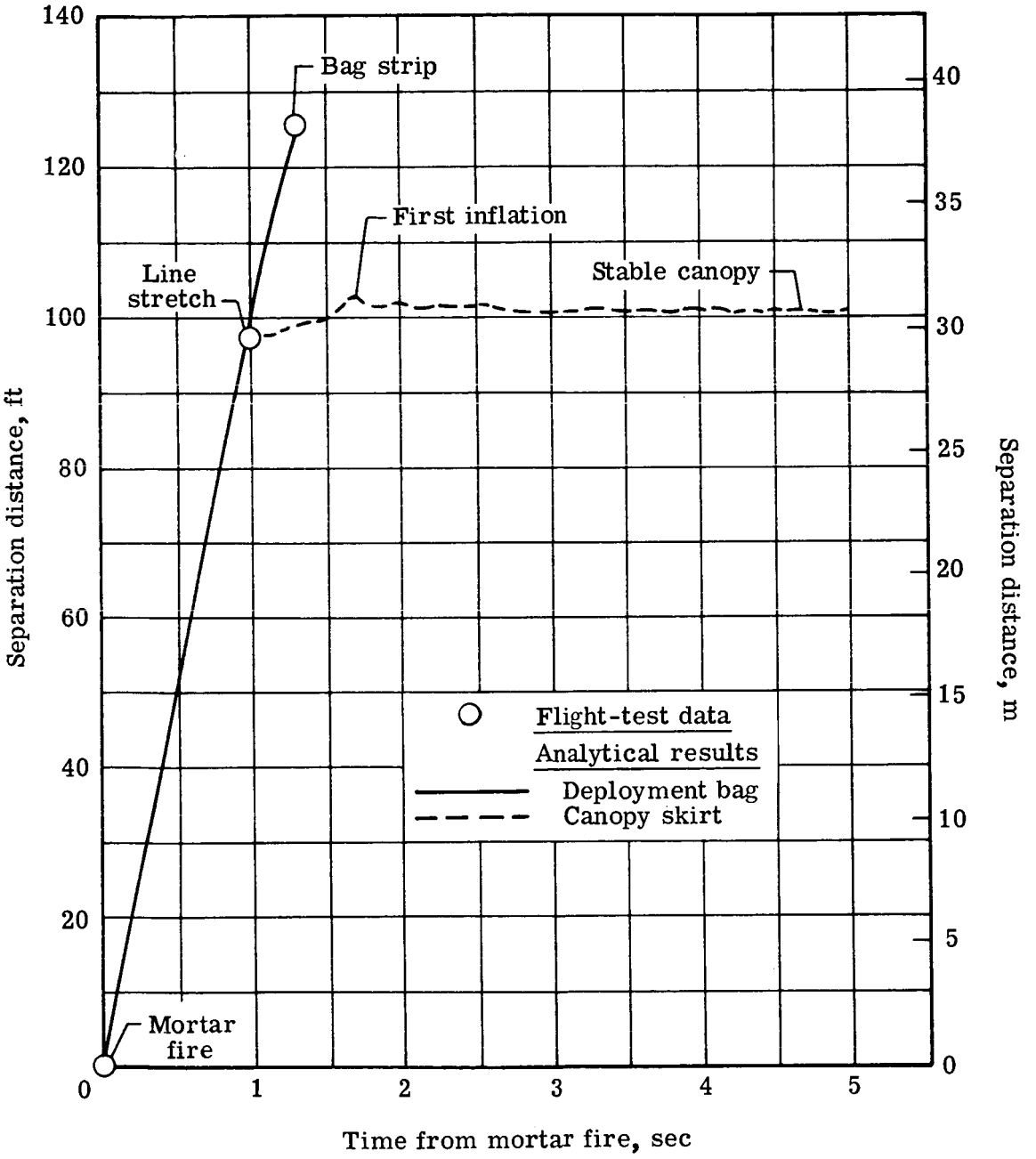

(a) BLDT AV-2.

Figure 4.- Simulation of separation distances (measured rearward from test vehicle) of deployment bag and canopy skirt.

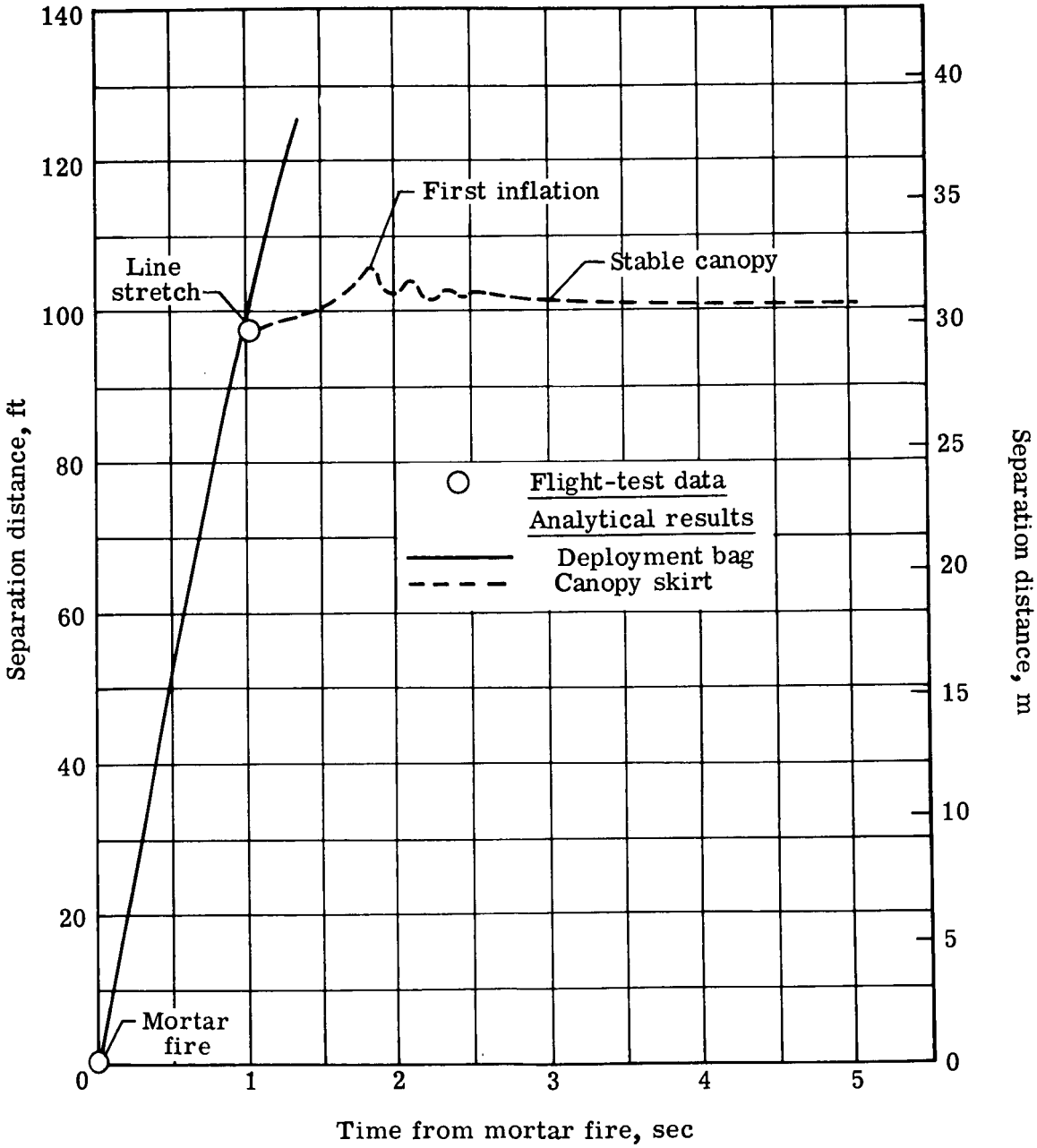

(b) BLDT AV-3.

Figure 4.- Continued.

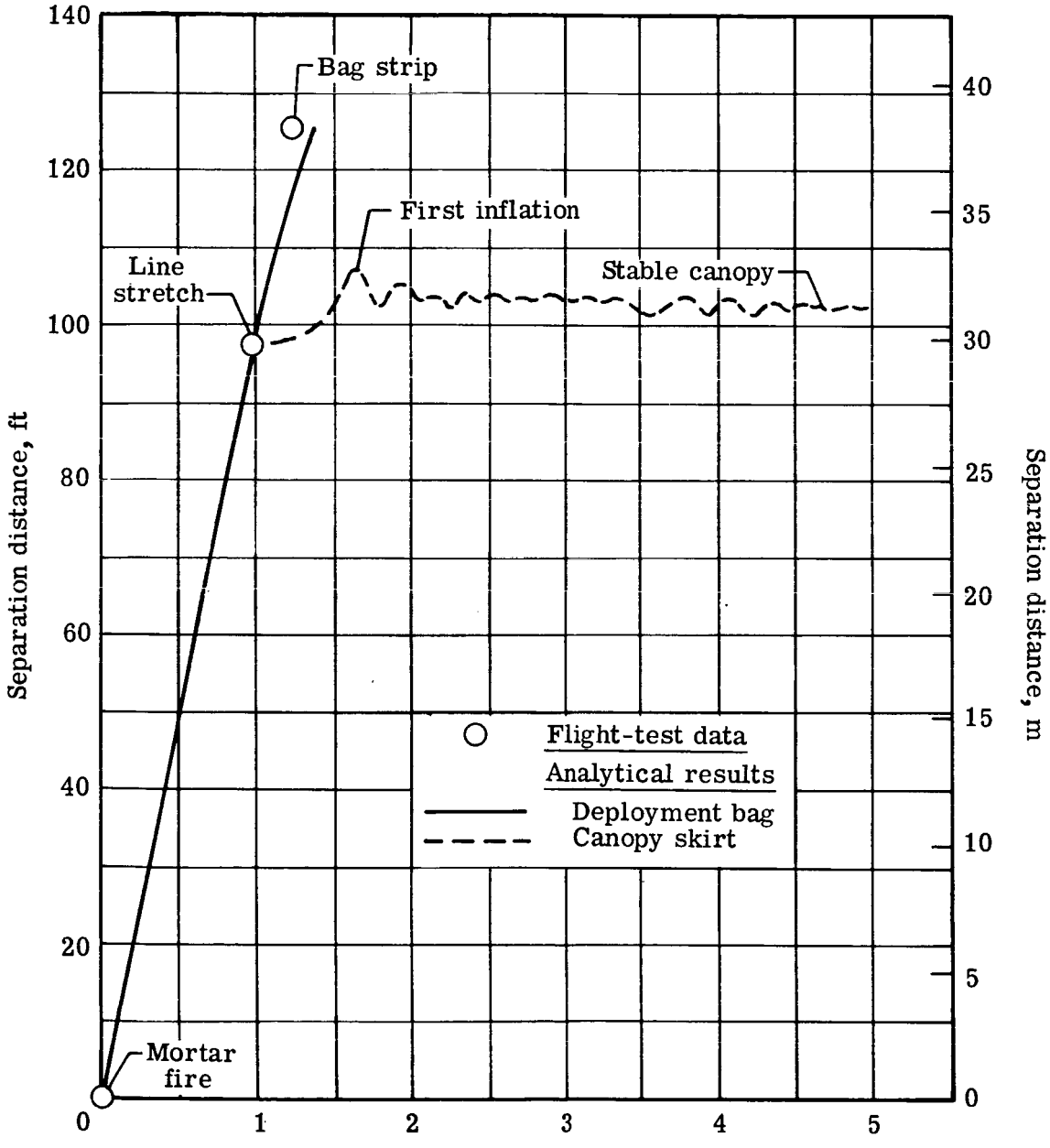

(c) BLDT AV-4.

Figure 4.- Continued.

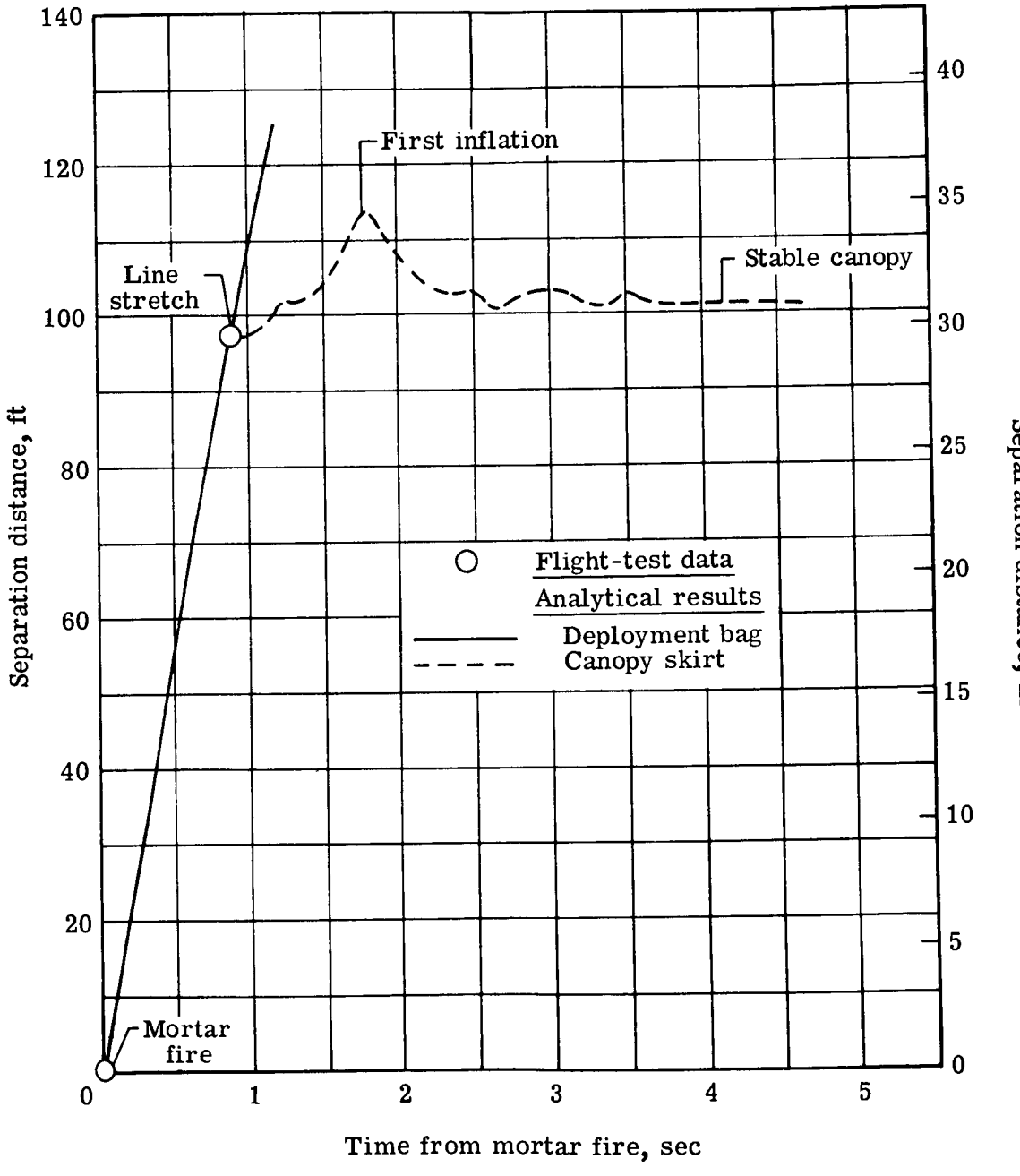

(d) LAQT-2.

Figure 4.- Continued.

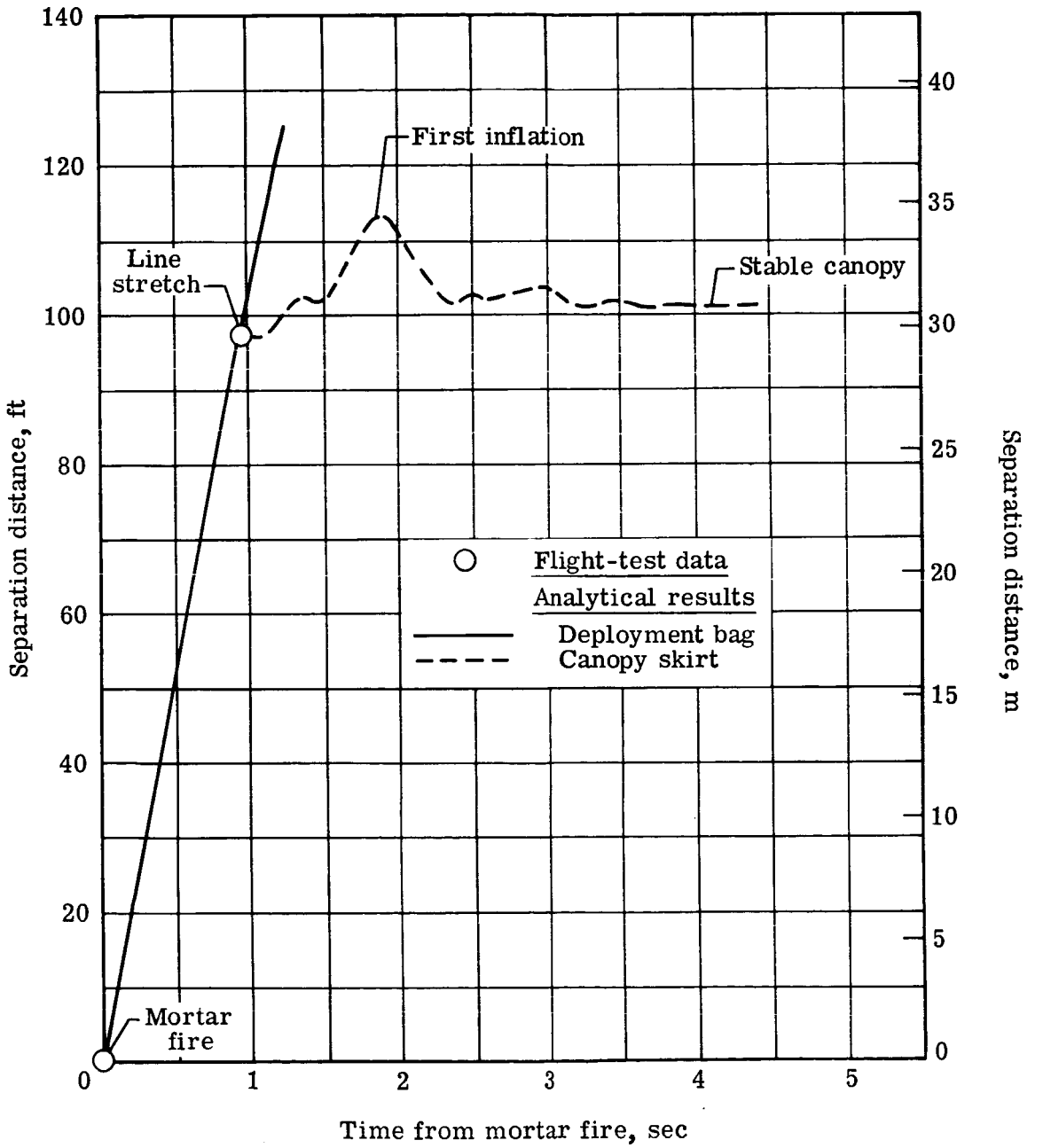

(e) LAQT-3.

Figure 4.- Concluded.

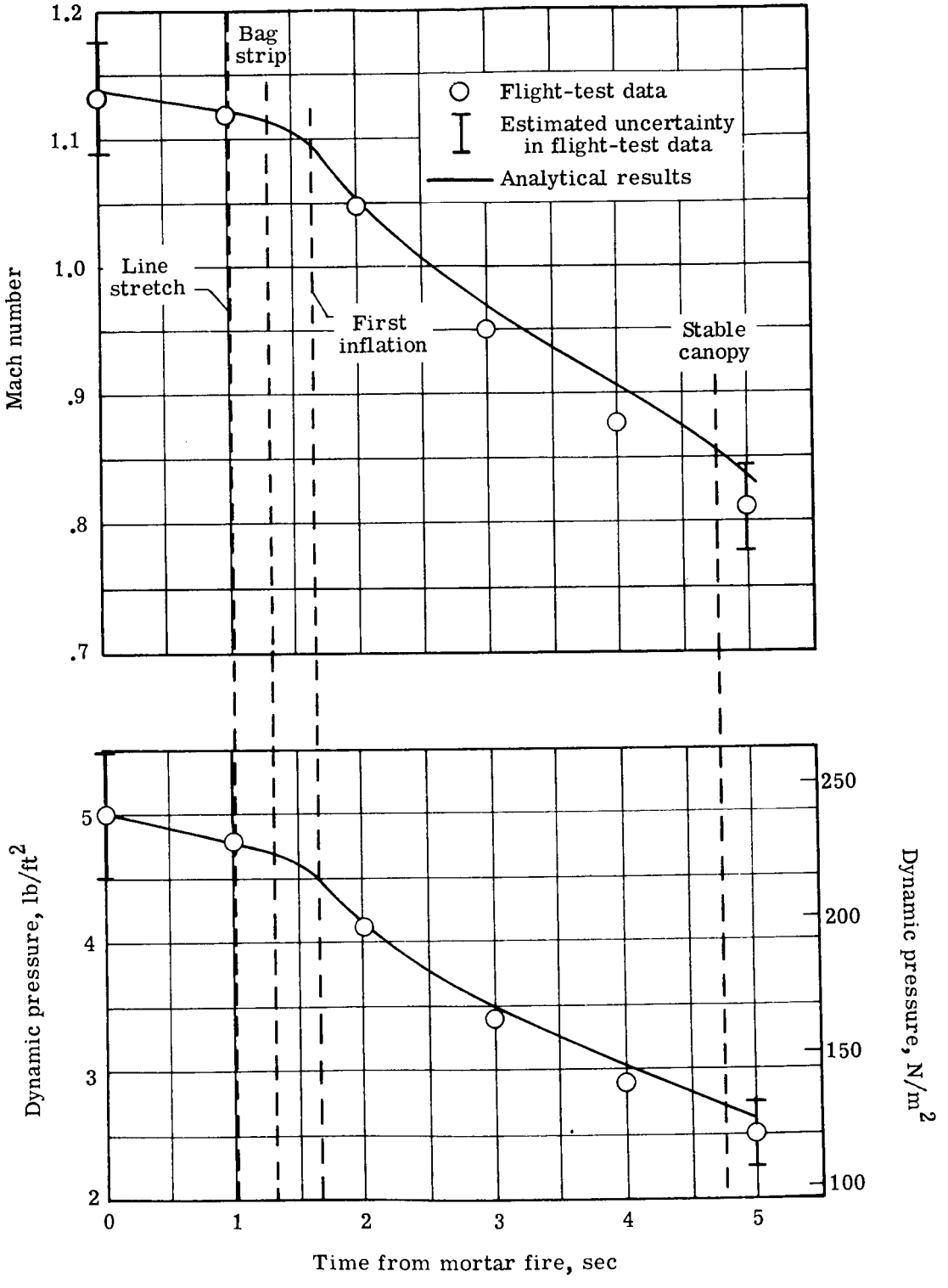

(a) BLDT AV-2.

Figure 5.- Simulation of free-stream Mach number and dynamic pressure.

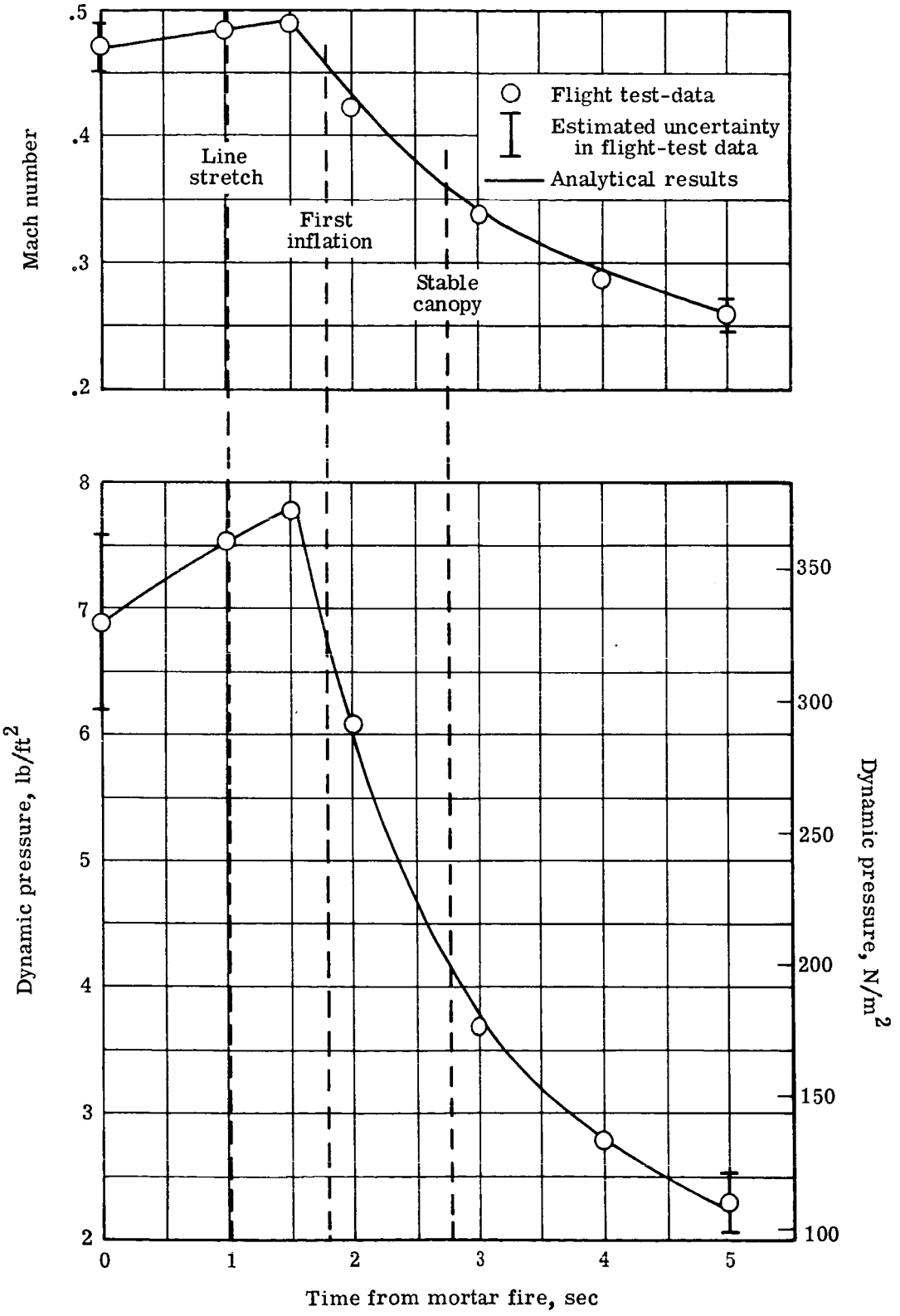

(b) BLDT AV-3.

Figure 5.- Continued.

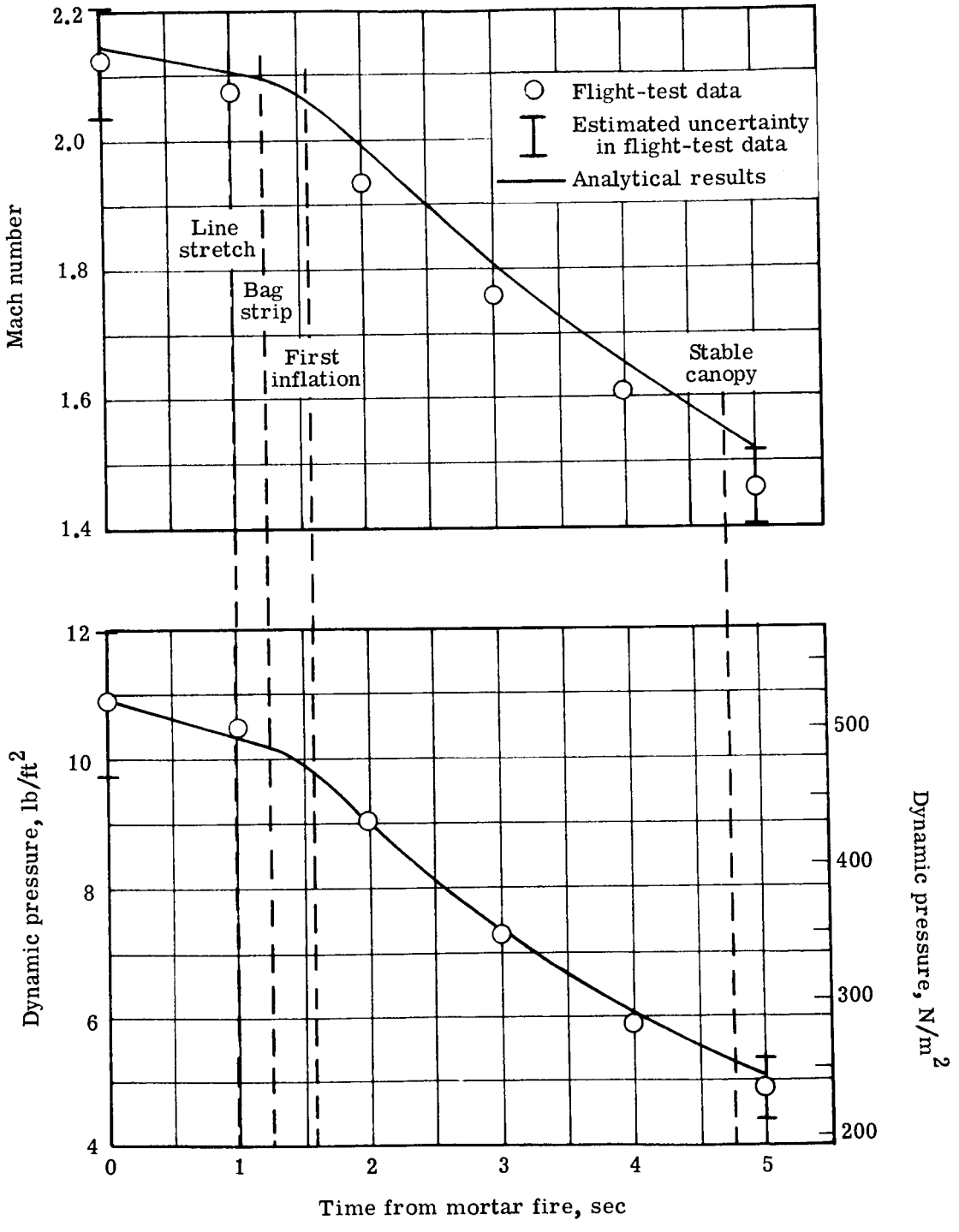

(c) BLDT AV-4.

Figure 5. - Continued.

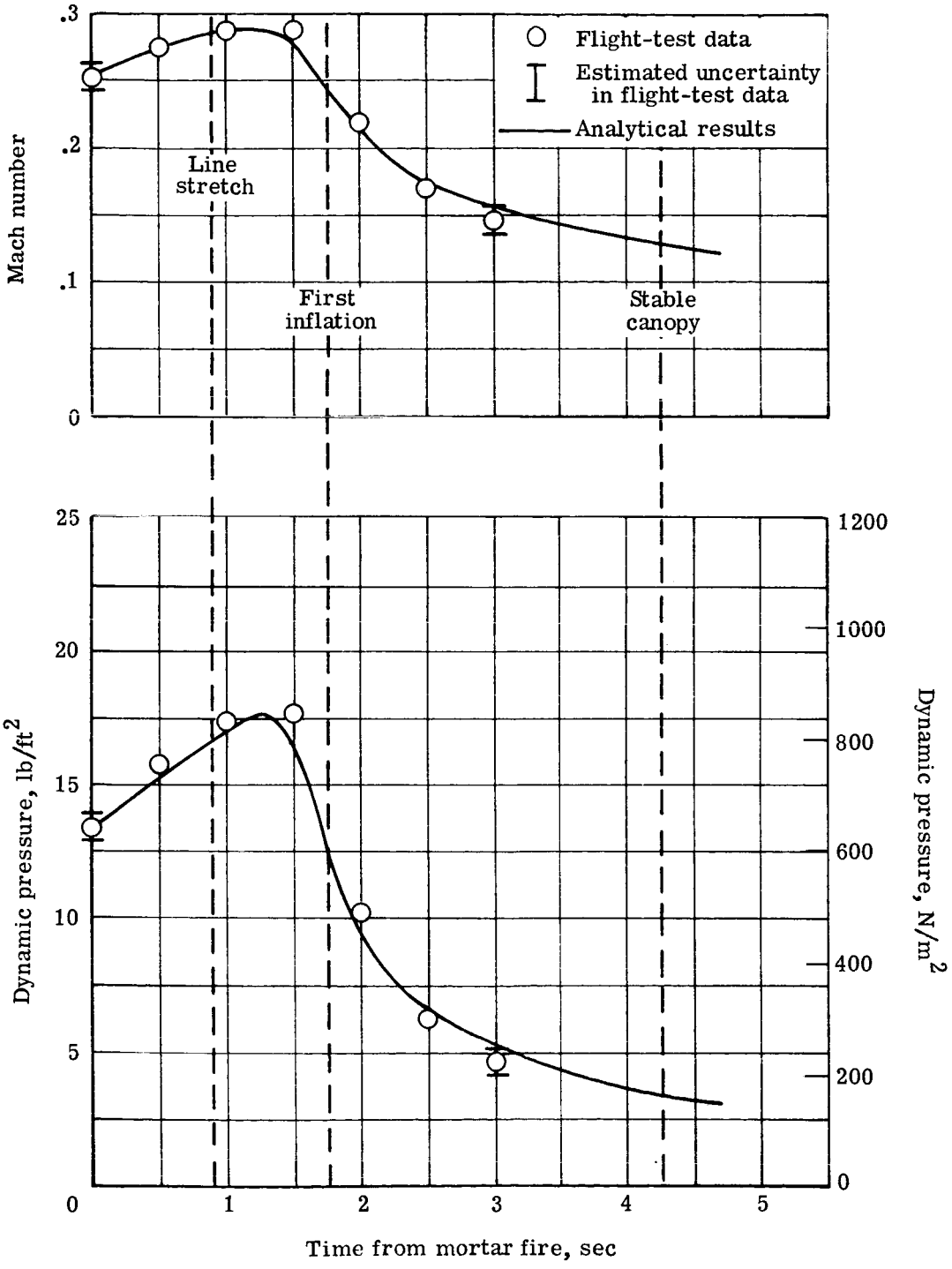

(d) LAQT-2.

Figure 5.- Continued.

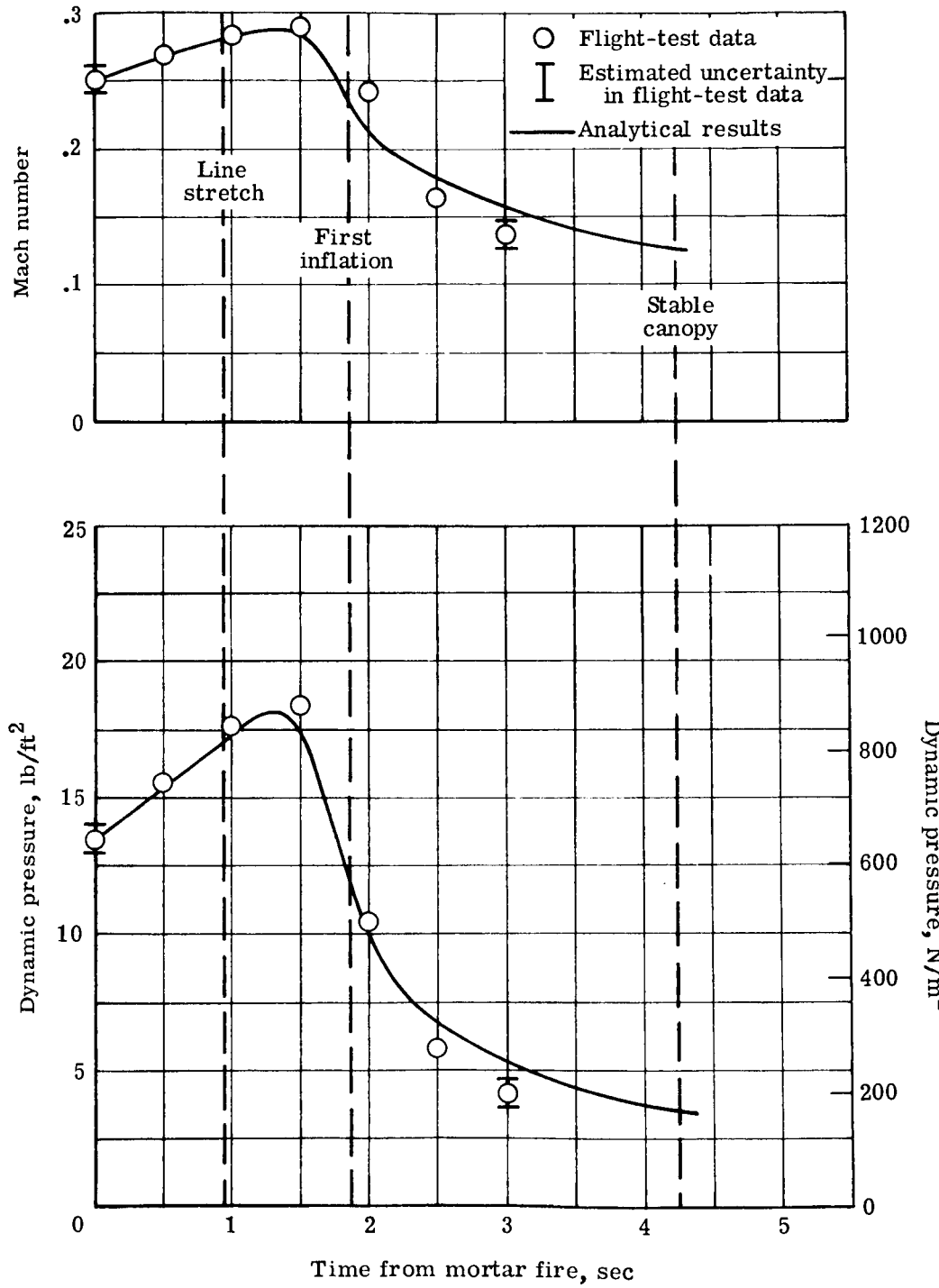

(e) LAQT-3.

Figure 5.- Concluded.

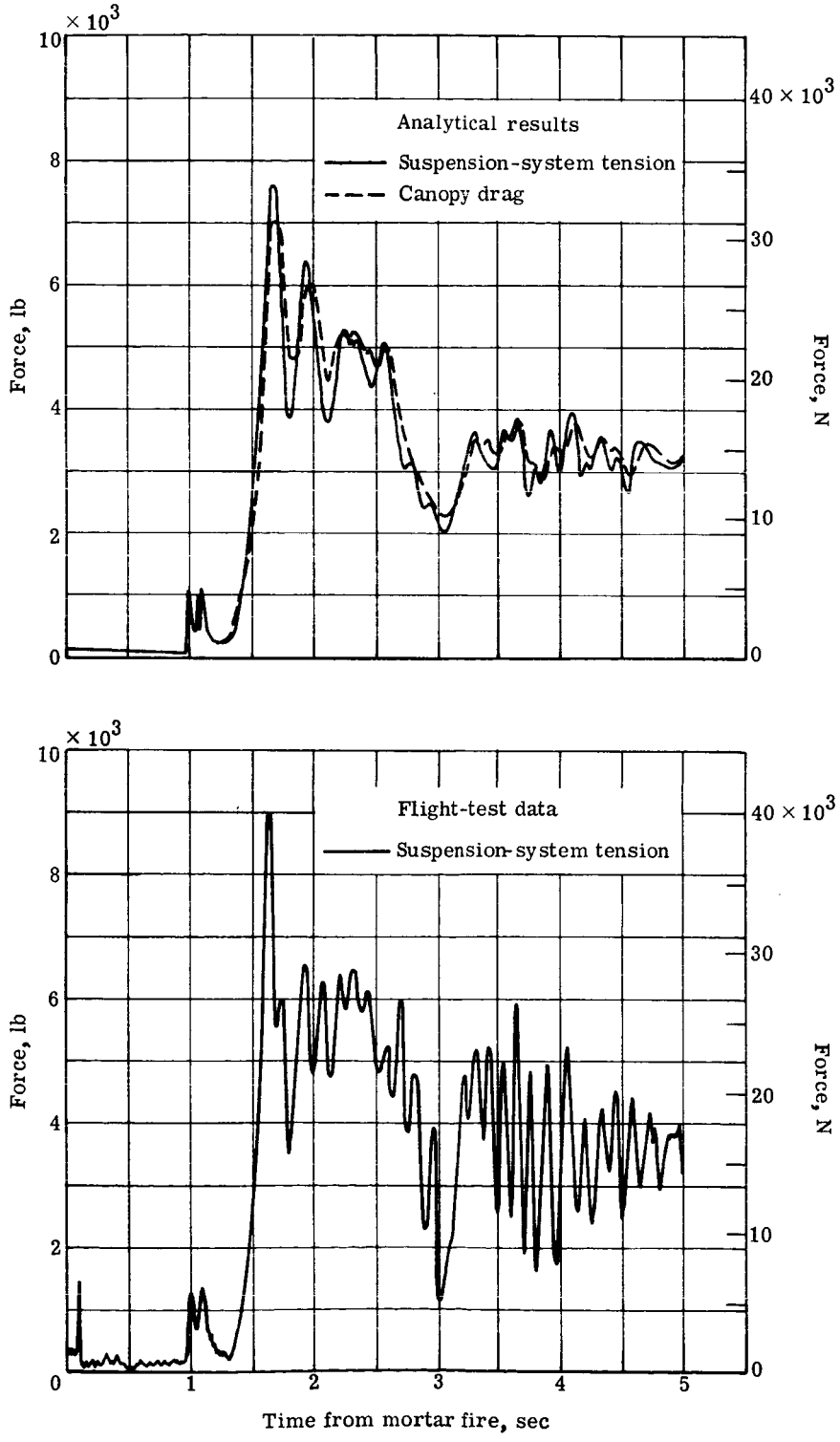

(a) BLDT AV-2.

Figure 6.- Simulation of suspension-system tension and canopy drag.

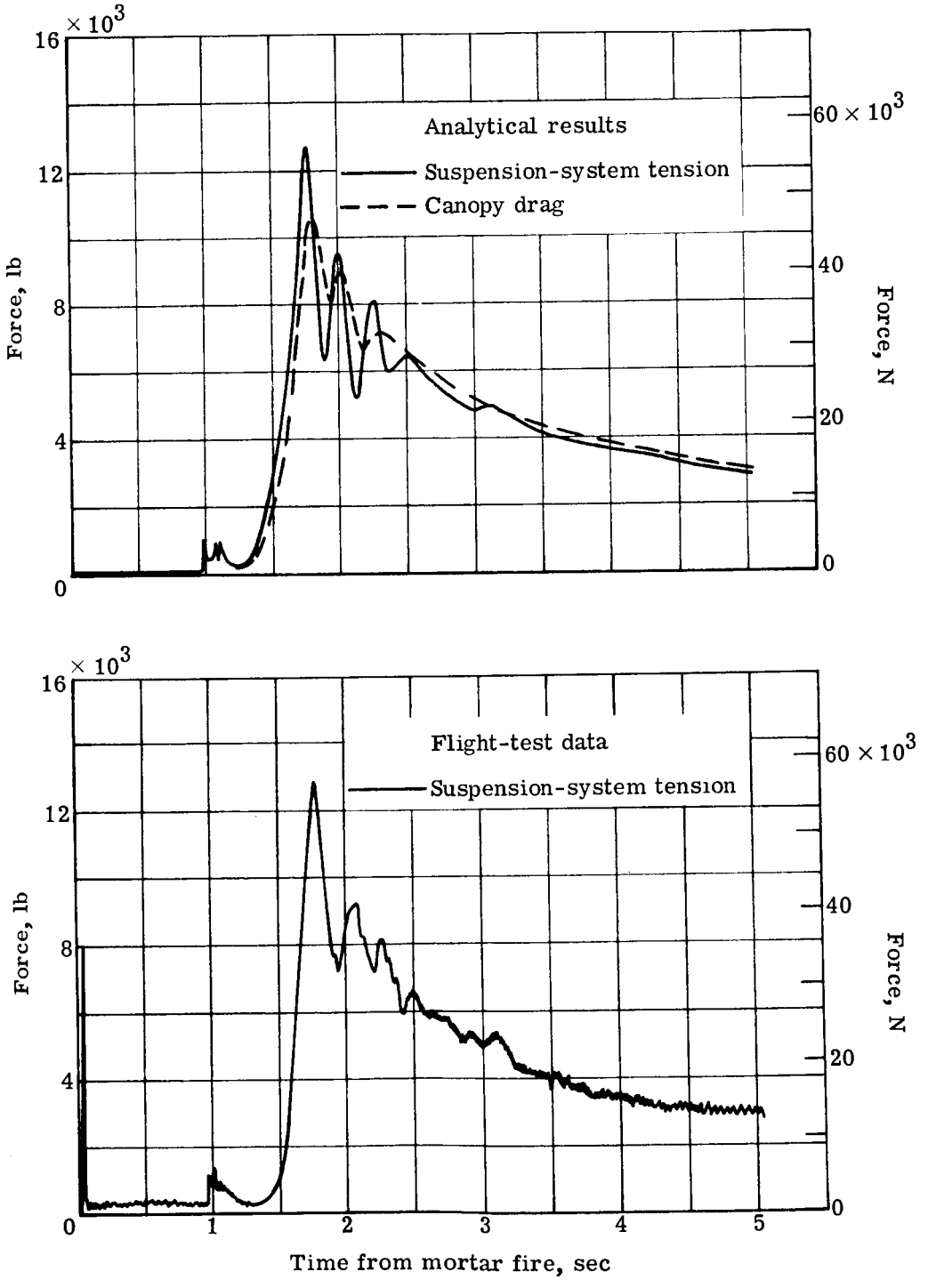

(b) BLDT AV-3.

Figure 6.- Continued.

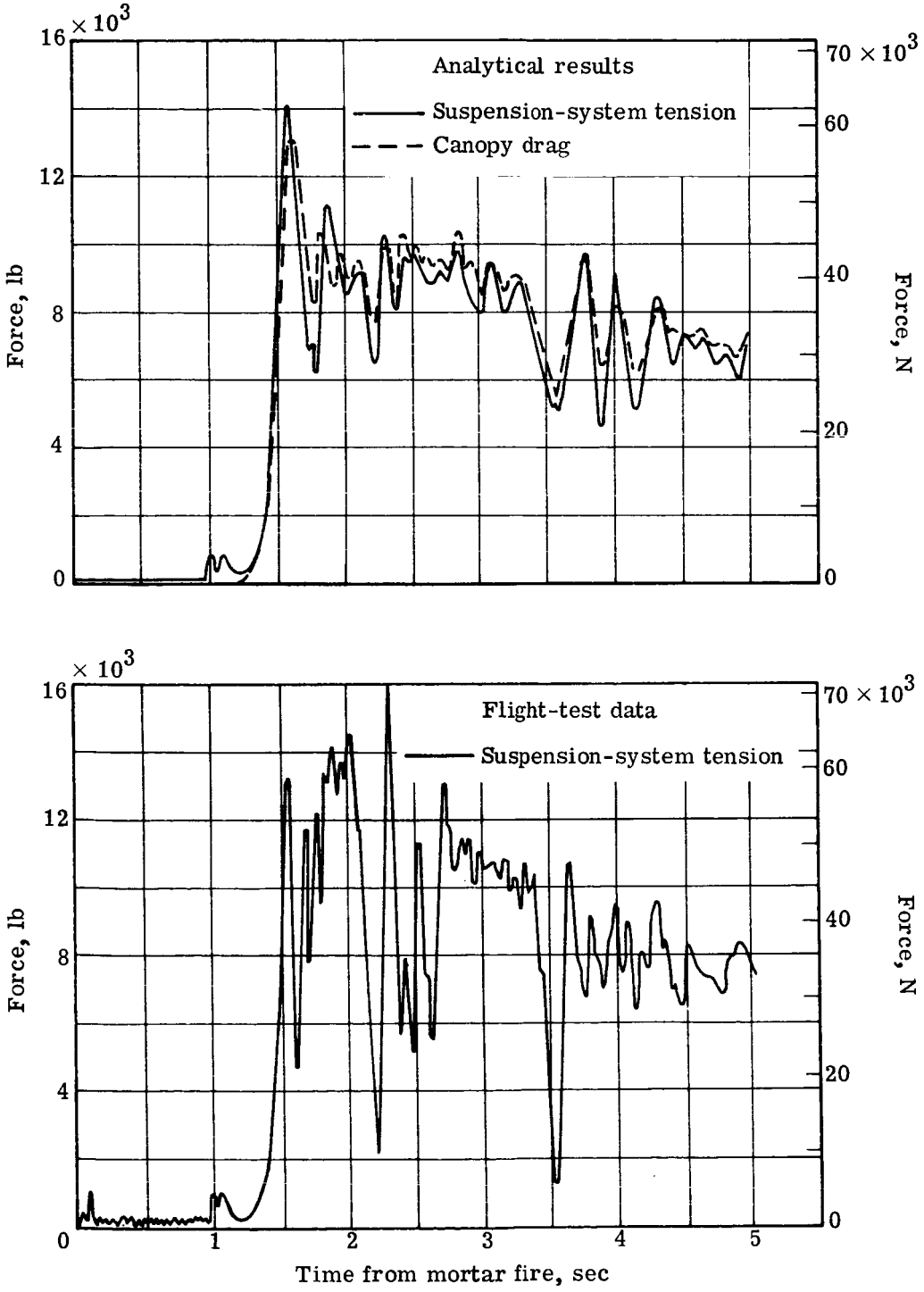

(c) BLDT AV-4.

Figure 6.- Continued.

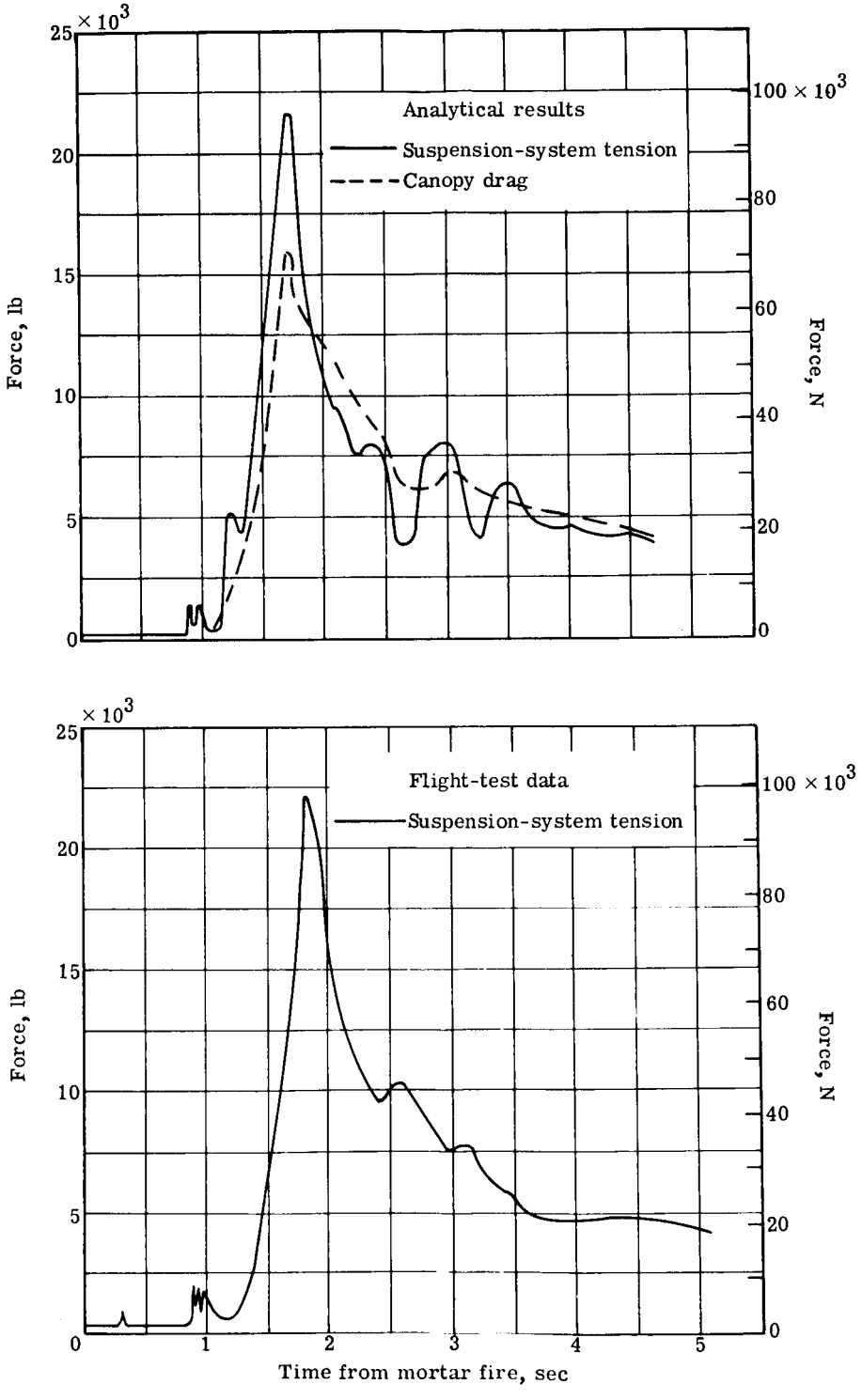

(d) LAQT-2.

Figure 6.- Continued.

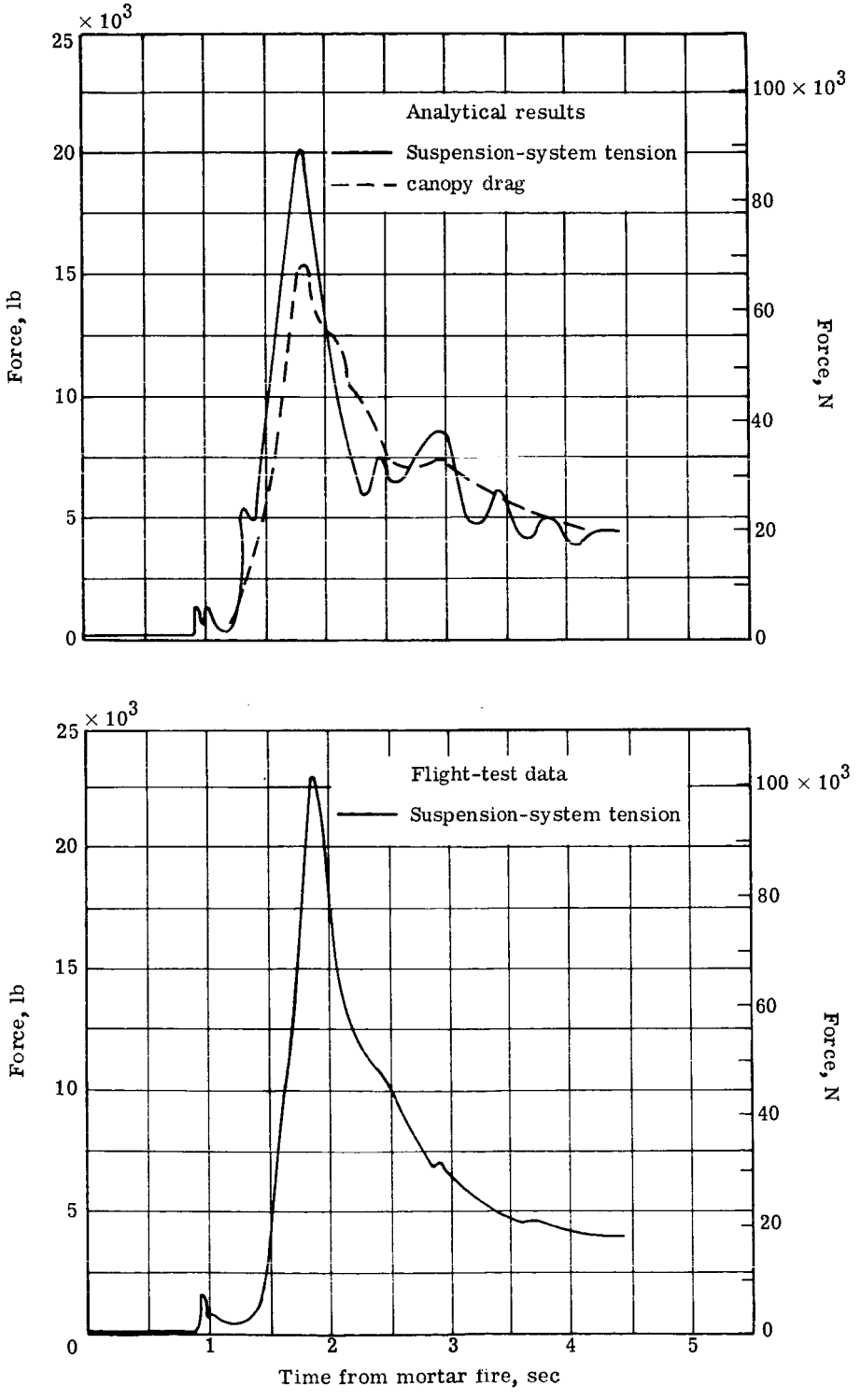

(e) LAQT-3.

Figure 6.- Concluded.

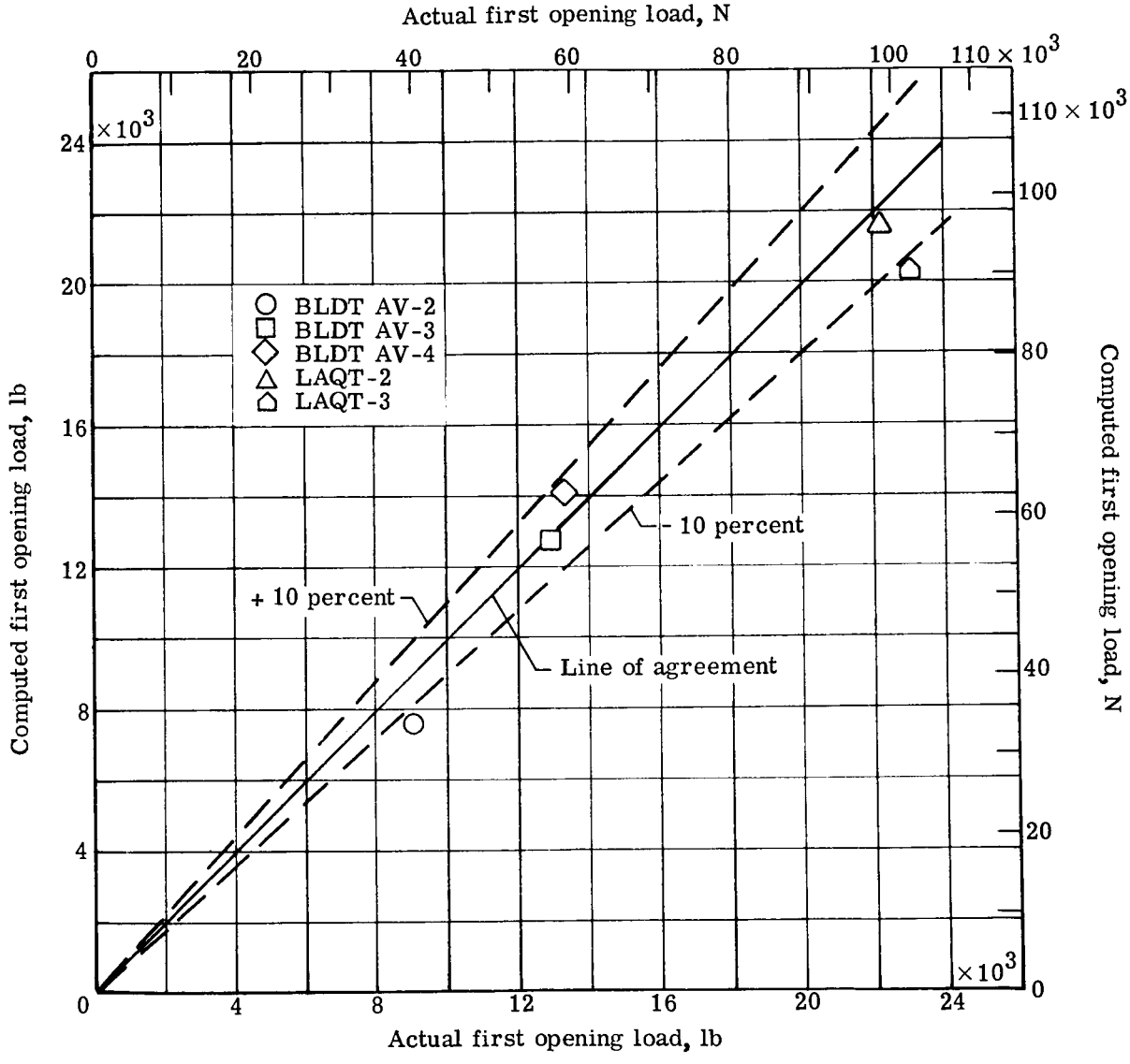

Figure 7.- Comparison of computed and actual first opening loads.

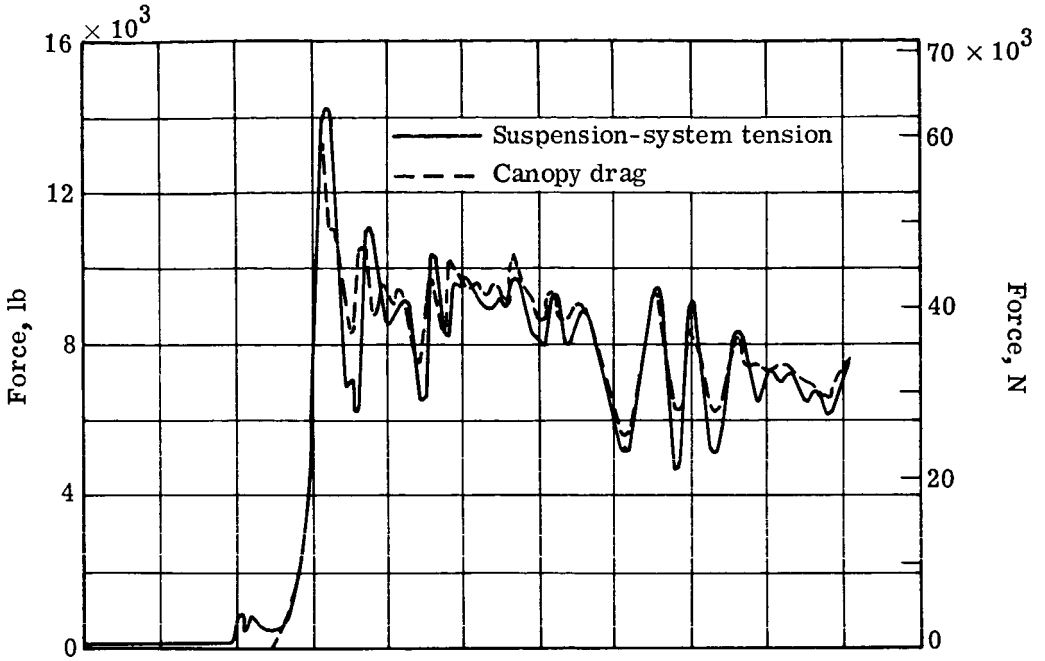

(a) Two-degree-of-freedom models (refs. 1 and 2).

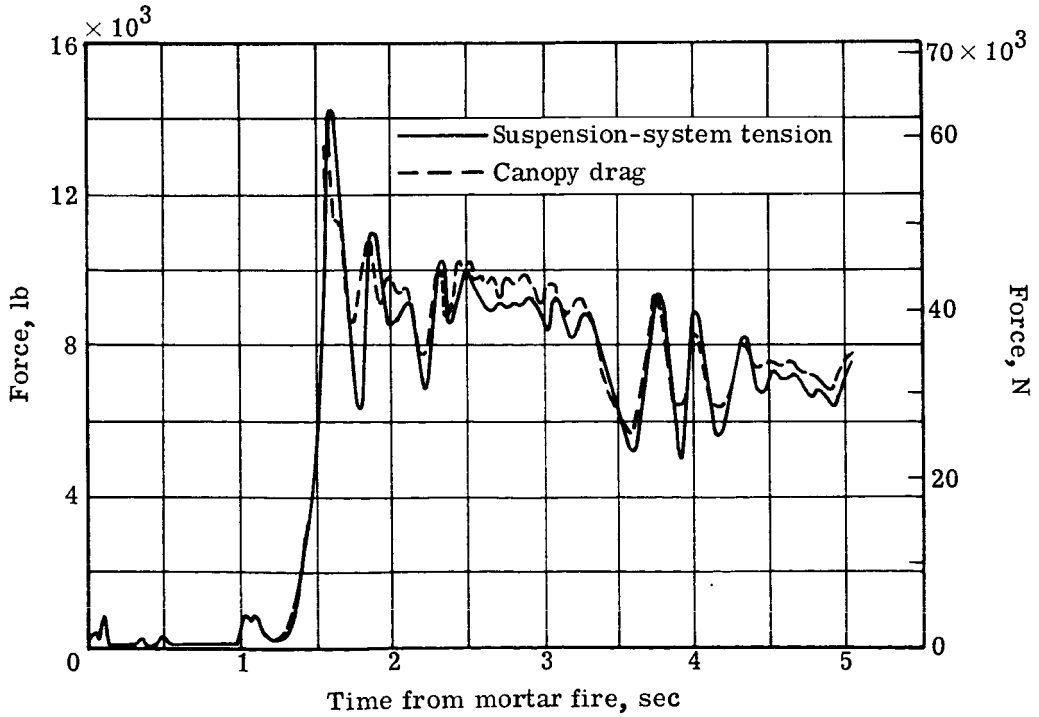

(b) Six-degree-of-freedom model (ref. 3).

Figure 8.- Comparison of computed force histories using different analytical models (AV-4 case).

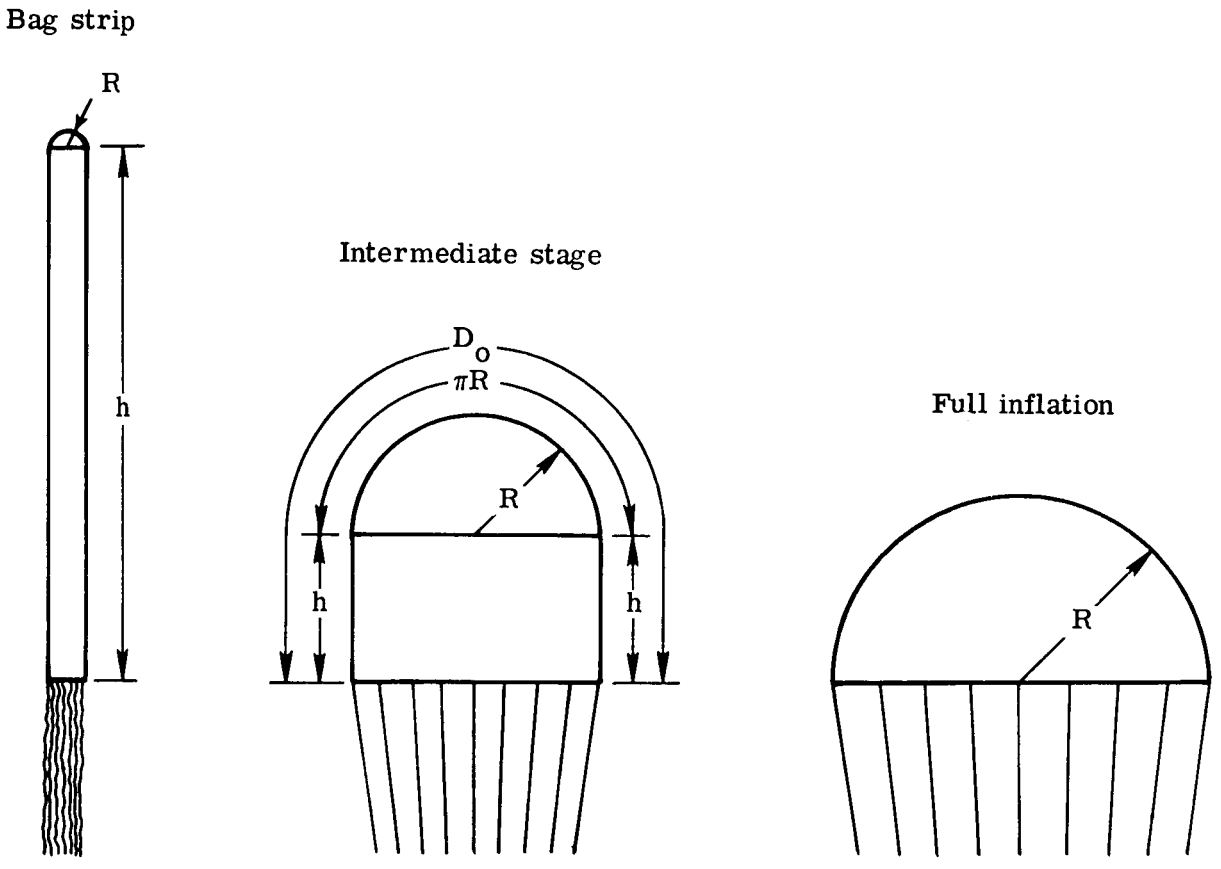

Figure 9.- Cylinder-hemisphere canopy model.

NASA-Langley, 1973 —— 31 L-9145